Hydrological variability in Florida Straits during Marine Isotope Stage 5 cold events

André Bahr,[1,2] Dirk Nürnberg,[1] Joachim Schönfeld,[1] and Dieter Garbe-Schönberg[3]

Received 22 June 2010; revised 12 January 2011; accepted 24 February 2011; published 21 May 2011.

[1] Modeling and proxy studies indicate that a reduction of Atlantic Meridional Overturning Circulation (AMOC) strength profoundly impacts temperatures and salinities in the (sub)tropical Atlantic, especially on subsurface levels. While previous studies focused on prominent periods of AMOC reduction during the last deglaciation, we aim to test whether similar reconfigurations of the subtropical hydrography occurred during the moderate climatic alterations punctuating the last interglacial Marine Isotope Stage (MIS) 5. Here, we present temperature and salinity records from a Florida Straits core by combining δ^{18}O and Mg/Ca analyses on surface (*Globigerinoides ruber*, white) and deep-dwelling (*Globorotalia crassaformis*) foraminifera covering MIS 5 in high resolution. The data reveal increasing salinities at intermediate depths during interglacial cooling episodes, decoupled from relatively stable surface conditions. This probably indicates the spatial expansion of saline subtropical gyre waters due to enhanced Ekman downwelling and might also point to a changed density structure and altered geostrophic balance in Florida Straits. Notably, these oceanographic alterations are not consistently occurring during periods of AMOC reduction. The data suggest that the expansion of gyre waters into Florida Straits was impeded by the increasing influence of Antarctic Intermediate Water (AAIW) from MIS 5.5 to ~107 kyr BP. Afterward, increasingly positive benthic δ^{13}C values imply a recession of AAIW, allowing the temporary expansion of gyre waters into Florida Straits. We argue that the inferred transient subtropical salt accumulation and warm pool expansion might have played a pivotal role in reinvigorating meridional overturning and dampen the severity of interglacial cold phases.

Citation: Bahr, A., D. Nürnberg, J. Schönfeld, and D. Garbe-Schönberg (2011), Hydrological variability in Florida Straits during Marine Isotope Stage 5 cold events, *Paleoceanography*, *26*, PA2214, doi:10.1029/2010PA002015.

1. Introduction

[2] The penultimate interglacial Marine Isotope Stage (MIS) 5 is known as a period of comparatively stable climate at mid and high latitudes that was only interrupted by short cooling intervals [e.g., *Chapman and Shackleton*, 1999]. While there is ample evidence for reduced deep Atlantic Meridional Overturning Circulation (AMOC) during those cooling episodes [e.g., *Chapman and Shackleton*, 1999; *Curry and Oppo*, 2005], the knowledge of concomitant changes in the subsurface and intermediate water is sparse. Furthermore, most research on MIS 5 focused on the high northern latitudes, which are particularly sensitive to changes in the ocean and climate system [e.g., *Bauch and Kandiano*, 2007; *Bauch et al.*, 2000; *Helmke and Bauch*, 2003; *McManus et al.*, 2002]. High-resolution paleotime series from (sub)tropical oceans are less abundant, although proxy as well as modeling studies pointed out that the (sub) tropical ocean with its enormous heat and salt storage capacity plays a significant role in the oceanic and atmospheric circulation system [e.g., *Rühlemann et al.*, 1999; *Schmidt et al.*, 2004, 2006].

[3] The intention of this study is to reconstruct changes in the vertical upper ocean gradients in the Florida Straits, which is a key area in the AMOC surface path. Variations in the global ocean circulation are expected to have considerable effects on the hydrography of this important oceanic gateway. Modeling studies suggest that profound and complex changes will take place in the tropical and subtropical Atlantic when AMOC strength is reduced [*Chang et al.*, 2008; *Wan et al.*, 2009; *Zhang*, 2007]. The model results invoke a subsurface warming parallel to surface cooling between 0 and 20°N, but a general cooling in the (sub)tropics north of 20°N [*Chang et al.*, 2008], which was accompanied by a salinity increase in the northern hemisphere tropics [*Wan et al.*, 2010]. In order to test the model predictions, the focus of our study was to reconstruct subsurface temperature and salinity dynamics during interglacial cooling events in a conduit of the AMOC surface flow path, where different water masses from the tropical and subtropical Atlantic are encountered.

[1]Leibniz Institute for Marine Sciences IFM-GEOMAR, Kiel, Germany.
[2]Now at Institute of Geosciences, University Frankfurt, Frankfurt am Main, Germany.
[3]Institute of Geosciences, Christian-Albrechts-Universität zu Kiel, Kiel, Germany.

0883-8305/11/2010PA002015

[4] Today, the temperatures of intermediate waters in the Florida Straits range from 12 to 24°C. They are dominated by recirculated subtropical gyre waters of the western North Atlantic (Figure 1a), while surface (>24°C) and deep (<12°C) waters are predominantly of South Atlantic origin [*Schmitz and Richardson*, 1991]. Subtropical gyre water constitutes a several hundred meter thick pool of warm and saline water (Western North Atlantic Central Water, WNACW) that is the ultimate source of the Subtropical Underwater (SUW). Before entering the southern Florida Straits, the SUW forms a subsurface salinity maximum in the Gulf of Mexico, being vertically less extensive than the WNACW in the subtropical Atlantic (Figure 1c). The piling-up of water masses in the subtropical gyre in combination with the Coriolis force results in a geostrophic flow through Florida Straits [*Wüst*, 1924] imprinted in the tilted pycnoclines at Florida Straits (Figure 1d). We expect similar conditions as today to have been prevailed during MIS 5. To reconstruct the geostrophic flow in the past, *Lynch-Stieglitz et al.* [1999a] used benthic $\delta^{18}O$ records from both sides of Florida Straits, converted them into density gradients, and calculated the geostrophic transport. This approach showed a quite pronounced variability of the density structure in the Florida Straits during the past 20 kyrs [*Lund et al.*, 2006; *Lynch-Stieglitz et al.*, 1999a, 2009], in particular less tilted pycnoclines during the Last Glacial Maximum, interpreted to represent a significantly reduced glacial Gulf Stream strength [*Lynch-Stieglitz et al.*, 1999a].

[5] In this study, we present the first surface and intermediate water temperature and salinity ($\delta^{18}O_{sw}$) records from Florida Straits that cover MIS 5 at high temporal resolution. We will demonstrate that a tight but complex coupling prevailed between northern hemisphere atmospheric changes and hydrographic variations in Florida Straits.

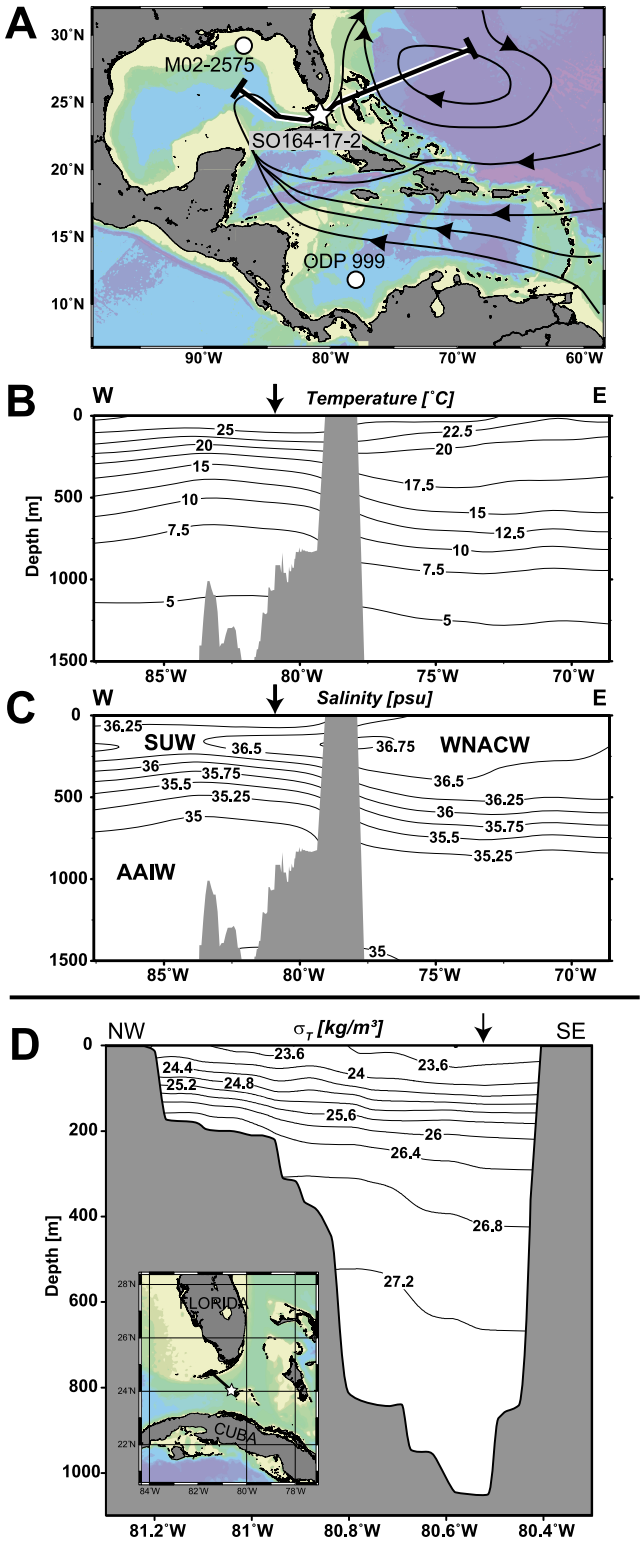

Figure 1. (a) Bathymetric map of the Caribbean and Gulf of Mexico with the position of core SO164-17-2 (star) and reference sites ODP 999 and MD02–2575 (circles) indicated. The dominant upper ocean circulation pattern (i.e., >7°C water) is drawn after *Schmitz and McCartney* [1993]. (b) Temperature and (c) salinity distribution along a transect from the central Gulf of Mexico to the western subtropical Atlantic (location of the transect as shown in Figure 1a). Water masses discussed in the text are shown in the hydrographic sections (AAIW, Antarctic Intermediate Water; SUW, Subtropical Underwater; WNACW, Western North Atlantic Central Water). (d) Hydrological cross section from Florida Keys to Cay Sal Bank showing the present-day isopycnals (σ_T, data from WOA09; http://www.nodc.noaa.gov/OC5/WOA09/pr_woa09.html). The star on the map (inset) and the arrow on the hydrological section mark the location of SO164-17-2. Plots were made with Ocean Data View 3.4.3 by Reiner Schlitzer (http://odv.awi.de).

2. Material and Methods

2.1. Core Selection and Sampling

[6] Quaternary sediments in the southern Florida Straits comprise foraminiferal oozes on the slope off Florida Keys, calcareous clays with intercalations of carbonate sand turbidites in the trough center, and patchy veneers of pteropod sands in the northeastern sector between Florida, Cay Sal, and Great Bahama Banks. Winnowing and redeposition is common, and sedimentation rates generally decrease from west to east [*Brunner*, 1986]. On R/V Sonne Cruise SO164, we discovered a mud patch between 700 and 1100 m depth on the northern slope to the northwest of Cay Sal Bank [*Nürnberg et al.*, 2003]. This patch is fringed by carbonate

sands and hardgrounds. Earlier hydrographic investigations revealed that the Florida Current is funneled in this area and occupies the entire cross section of the Strait down to 800 m water depth [*Richardson et al.*, 1969]. Sediments from this mud patch therefore recorded the properties of surface and subsurface water masses of the Florida current and the influence of underlying intermediate water masses during the geological past.

[7] Piston core SO164-17-2 was recovered during R/V *Sonne* Cruise SO164 from this mud patch in the southern Florida Straits (24°04.99′N; 80°53.00′W; 954 m water depth; Figure 1). The core is 1172 cm long and comprises a uniform succession of carbonaceous olive gray to gray sandy and silty clay. Sedimentary textures indicating winnowing or redeposition were not recognized despite two layers of fine carbonate sand with a fining upward gradation, which were encountered at 790 and 1021 cm, far below the interval considered in this study. Bulk sediment samples, in particular half-core slices with a thickness of 1.5 cm were taken every 2 cm from the core top to 180 cm, and every 4 cm at depths below. The sample resolution was later refined to 2 cm in the MIS 5 interval down to 480 cm by using 10 cm^3 cutoff syringes of 1.5 cm diameter. The samples were freeze dried and washed through a 63 μm screen. The residues were dried at 60°C, weighed, and further subdivided into different size fractions by dry sieving.

2.2. Sample Preparation

[8] After freeze drying, wet sieving, and fractionation, 30 specimens of *Globigerinoides ruber* (white variety) and *Globorotalia crassaformis* were picked from the 315–355 μm fraction as a pooled sample for stable isotope and Mg/Ca analysis. In the case of *G. crassaformis*, the size fraction for combined $\delta^{18}O$ and Mg/Ca analysis was occasionally extended to 355–400 μm in order to achieve the required amount of carbonate for the analyses. In few cases, we also sampled the 250–315 and >400 μm fraction, but because of the size dependence of the Mg/Ca paleothermometer [*Elderfield et al.*, 2002], we used *G. crassaformis* specimens from these fractions only for stable isotope analyses. Shells were gently crushed between two glass plates to open the chambers, mixed with a brush in order to achieve a homogenized sample and then divided into subsamples constituting a third of the total amount for stable isotope analyses and two thirds for Mg/Ca measurements.

2.3. Stable Isotope Analyses and Radiocarbon Dating

[9] Subsamples for stable isotope analyses of planktic foraminifera were rinsed three times with ultrapure water and methanol. For the benthic isotope record 1–3 tests of *Cibicidoides wuellerstorfi* were selected from the 250–400 μm size fraction. In addition, 20 specimens of *Globigerinoides sacculifer* were picked from the 315–400 μm fraction to establish an initial oxygen isotope stratigraphy for the whole core. Stable isotope samples were run on Finnigan MAT 252 and Thermo Fisher Scientific 253 Mass Spectrometers with automated carbonate preparation devices. Analytical long-term precision (n = >1000 analyses) based on an internal standard referenced to the NBS 19 standard was <0.06‰ for $\delta^{18}O$ and <0.03‰ for $\delta^{13}C$. Replicate measurements yielded an external reproducibility of $\delta^{18}O$ values of ±0.10‰ (n = 5) for *G. ruber* (w) and ±0.20‰ (n = 18) for *G. crassaformis* (1σ values).

[10] For ^{14}C dating, 695 to 800 tests of *G. ruber* (w) were picked from the >250 μm size fractions of 9 samples between 4 and 40 cm core depth. Radiocarbon ages were determined via accelerator mass spectrometry (AMS) at the Leibniz-Labor of Kiel University. The precision of the ^{14}C ages ranged from ±25 to +360/−370 years (1σ). Carbon-14 ages younger than 24 ka BP were transferred to calendar years by using the Calib 5.02 program with MARINE04 calibration curve. For older datings, we used the CalPal Online calendar year correction program (CalPal2007_HULU calibration curve). An ocean reservoir correction of 400 yr was applied to all calibrated ages.

2.4. Foraminiferal Mg/Ca Cleaning and Analyses

[11] For Mg/Ca analysis the crushed subsamples were treated following the cleaning protocol of *Barker et al.* [2003] without a reductive cleaning step and analyzed using a simultaneous, radially viewing ICP-OES (Ciros CCD SOP, Spectro A.I., Germany) with a cooled cyclonic spraychamber in combination with a microconcentric nebulizer (200 μL/min sample uptake) optimized for best analytical precision and minimized uptake of sample solution. Sample introduction was performed via an autosampler (Spectra A.I.). For Ca, we used the 307.603 nm spectral line, while for Mg the 279.553 nm line was chosen. Matrix effects caused by varying concentrations of Ca were found to be insignificant as long as Ca concentrations are within the range of 20–80 ppm. To correct for machine offsets, we normalized the data relative to the ECRM 752–1 standard applying a Mg/Ca ratio of 3.762 mmol/mol according to *Greaves et al.* [2008] and corrected for analytical drift using the ECRM 752–1 as an internal consistency standard every 10 samples. Due to the small volume of our sample solutions, we were able to run only a limited amount of duplicate analyses yielding a standard deviation for Mg/Ca of 0.17 mmol/mol (*G. ruber* (w), n = 12, equals ±0.4°C) and 0.11 mmol/mol (*G. crassaformis*, n = 23, equals ±0.5°C), respectively.

2.5. Temperature Calculation

2.5.1. Sea Surface Temperatures

[12] Calculation of sea surface temperatures (SST) from $Mg/Ca_{G.ruber}$ was done following the multispecies equation provided by *Anand et al.* [2003] (1), which is based on a sediment trap study in the Sargasso Sea in the western subtropical Atlantic:

$$Mg/Ca[\mathrm{mmol/mol}] = 0.38(\pm 0.02)\exp(0.090(\pm 0.003)\mathrm{SST}[^{\circ}\mathrm{C}]). \quad (1)$$

We chose this equation as it is based on the same cleaning protocol and has a lower error than the single-species calibration of *Anand et al.* [2003].

[13] The multispecies equation (1) has been used before to create other records from Florida Straits [*Lund et al.*, 2006] and the Gulf of Mexico [*Nürnberg et al.*, 2008]. This secures the comparability of the different records.

[14] The average Holocene $SST_{Mg/Ca}$ values of 29.1 ± 0.4°C (see Data Set S1 in the auxiliary material) are warmer

than present annual mean SSTs (26.5–27°C [*Locarnini et al.*, 2006]) but are in the range of today's summer temperatures [*Locarnini et al.*, 2006], pointing at a summer bias in the $SST_{Mg/Ca}$ record.[1] MIS 5.5 $SST_{Mg/Ca}$ are 2 to 3°C higher than Holocene $SST_{Mg/Ca}$ (Figure 2d), which is in line with other records from the Gulf of Mexico (MD02–2575 *Nürnberg et al.* [2008]) and Caribbean (ODP 999 *Schmidt et al.* [2004]). It should be noted that MIS 5.5 temperatures as high as 32.5°C are on the upper limit of the applied calibration, introducing an additional uncertainty for $SST_{Mg/Ca}$ reconstructions.

2.5.2. Intermediate Water Depth Temperatures

[15] Intermediate water depth temperatures ($IWT_{Mg/Ca}$) were calculated using the multispecies calibration equation for deep-dwelling foraminifera by *Regenberg et al.* [2009] (2) based on core tops from the tropical Atlantic and Caribbean:

$$\mathrm{Mg/Ca[mmol/mol]} = 0.38(\pm 0.02)\exp(0.09(\pm 0.003)\mathrm{SST[^{\circ}C]}. \quad (2)$$

The Holocene $IWT_{Mg/Ca}$ was on average 11.3±1.3°C (see Data Set S1 in the auxiliary material), which agrees with the proposed calcification depth of *G. crassaformis* at ~400 m [*Steph et al.*, 2009] (Figure 1b). The single-species equation for *G. crassaformis* by *Anand et al.* [2003] as well as the multispecies equation by the same authors yield consistently higher temperatures (Holocene mean = 20.2, and 18.7°C, respectively). The equation by *Regenberg et al.* [2009] is better constrained for deep-dwelling foraminifera, especially *G. crassaformis*, due to the higher number of samples included (45 samples of *G. crassaformis* in the work of *Regenberg et al.* [2009] compared to 17 in the work of *Anand et al.* [2003]) and the wider range of Mg/Ca ratios covered (1.4–2.6 mmol/mol in the work of *Regenberg et al.* [2009], which is extended to 3.3 mmol/mol when including *G. truncatulinoides*, compared to 1.3–2.1 mmol/mol for *G. crassaformis* in the work of *Anand et al.* [2003]).

2.6. Calculation of $\delta^{18}O_{ivf\text{-}sw}$

[16] Sea surface and intermediate water depth salinities can be approximated by computing $\delta^{18}O_{ivf\text{-}sw\ (ice\ volume\text{-}free\ seawater)}$. For better comparison with published records [*Nürnberg et al.*, 2008; *Schmidt et al.*, 2004] we used the procedure published by *Schmidt et al.* [2004], where $\delta^{18}O_{ivf\text{-}sw}$ is derived from the combination of Mg/Ca temperatures and $\delta^{18}O$ measurements applying the $\delta^{18}O$ temperature relation of *Thunell et al.* [1999] and a correction for the global ice-volume signal following *Waelbroeck et al.* [2002]. Although the present-day linear relationship between salinity and $\delta^{18}O_{water}$ is well constraint for the Florida Straits [e.g., *Lynch-Stieglitz et al.*, 1999b] we restrain from calculating salinities for MIS 5 with this regression. The $\delta^{18}O$ salinity relation is likely to have changed through time due to different hydrological conditions altering the end-member characteristics of mixing water masses. As discussed later, we expect shifts in (sub)tropical wind fields and concomitant variations in the evaporation/precipitation ratio over the subtropical gyre during MIS 5 that should have caused a different $\delta^{18}O$ salinity relationship for the surface ocean over time. At intermediate depths, the relative contribution of different water masses (i.e., the varying influence of AAIW and SUW) is hard to assess, but most likely will have affected the middle-depths $\delta^{18}O$-salinity relationship.

[17] Error propagation based on the uncertainty of the paleotemperature and $\delta^{18}O_{calcite}$ to $\delta^{18}O_{seawater}$ conversion equations and the reproducibility of the $\delta^{18}O$ and Mg/Ca measurements results in cumulative uncertainties of ±0.26‰ for the $\delta^{18}O_{seawater}$ of *G. ruber* (w) and ±0.35‰ for *G. crassaformis*. The amount of the additional error attributed to the ice volume correction with reference to age model uncertainties and the error of the ice volume estimates itself is difficult to assess. However, during the interval between MIS 5.1–5.4, which is considered in detail in this study, the amplitude of the $\delta^{18}O$ variations caused by ice volume changes were ~0.15‰ according to *Waelbroeck et al.* [2002], which is very low compared to the observed $\delta^{18}O$ anomalies in the *G. crassaformis* record.

[18] Please note that the data obtained on SO164-17-2 is presented in the auxiliary material (Data Sets S1–S4) and will be made available in the online database PANGAEA (www.pangaea.de).

3. Results and Discussion

3.1. Chronostratigraphy

[19] The stratigraphic reach of core SO164-17-2 was constrained with calcareous nannofossils and *Globorotalia menardii* biozones. A smear slide from the core base showed small *Gephyrocapsa* and *Emiliania huxleyi*. *Pseudoemiliania lacunosa* was not recorded, which infers the nannoplankton zone NN21 with a maximum age of 270 ka. The boundaries of Ericson zones Z, Y, X, W, and V [*Ericson and Wollin*, 1968] were determined by screening of the size fractions >250 μm for the first and last occurrences of *Globorotalia menardii* (Figure 3a and Data Set S3). The V/W boundary at 528 cm indicates that the record of the upper part of the core is complete and goes back beyond 165 ka [*Brunner*, 1984; *Peterson et al.*, 2000]. Ambiguous abundance fluctuations of *G. menardii* in the lower part of the core inhibit the recognition of older Ericson zone boundaries. A correlation of the planktonic oxygen isotope curve of *Globigerinoides sacculifer* (Figure 3b and Data Set S4) with records from ODP Site 1002 [*Haug et al.*, 2001; *Peterson et al.*, 2000] and stacked standard records [*Martinson et al.*, 1987] revealed that core SO164-17-2 comprises MIS 1 through 8 and goes back to 271.7 ka.

[20] The upper section of the core comprising the Holocene and last deglaciation was condensed, i.e., 18.8 kyrs were represented by 32 cm only. The following 2 cm comprise the entire Last Glacial Maximum as constrained by bracketing AMS ^{14}C datings (see Data Set S5 in the auxiliary material). No sharp or oblique contact was visible at this interval which would indicate an unconformity despite an indistinct color change from light gray to light cream. The top of the core is well preserved. If at all, only a few centimeters were missing as indicated by a dark seam of manganese oxides at 2 cm in core SO164-17-2, which was found between 5 and 6 cm sediment depth in box core SO164-17-1 from the same location. Even though the Holocene is apparently complete and well constrained in

[1] Auxiliary materials are available at ftp://ftp.agu.org/apend/pa/2010PA002015.

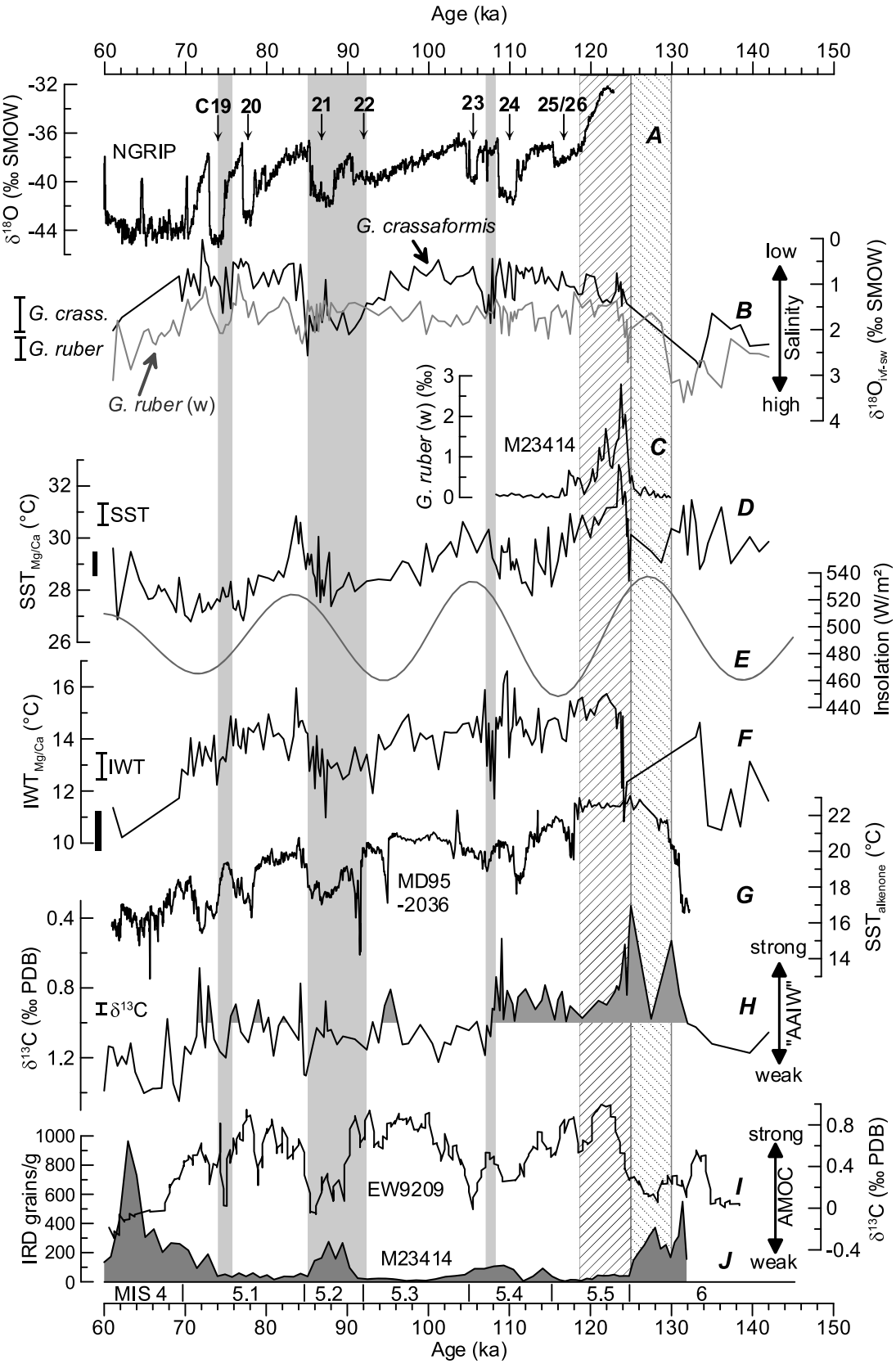
Age (ka)
60 70 80 90 100 110 120 130 140 150
δ18O (‰ SMOW)
-32 -36 -40 -44
C19 20 21 22 23 24 25/26
NGRIP
A
G. crassaformis
G. crass.
G. ruber
G. ruber (w)
low
Salinity
high
B
δ18Oivf-sw (‰ SMOW)
0 1 2 3 4
G. ruber (w) (‰)
0 1 2 3
M23414
C
SST
SSTMg/Ca (°C)
32 30 28 26
D
E
Insolation (W/m²)
540 520 500 480 460 440
IWT
IWTMg/Ca (°C)
16 14 12 10
F
MD95
-2036
G
SSTalkenone (°C)
22 20 18 16 14
δ13C
δ13C (‰ PDB)
0.4 0.8 1.2
strong
"AAIW"
weak
H
EW9209
I
M23414
J
IRD grains/g
1000 800 600 400 200 0
strong
AMOC
weak
0.8 0.4 0 -0.4
δ13C (‰ PDB)
MIS 4 5.1 5.2 5.3 5.4 5.5 6
60 70 80 90 100 110 120 130 140 150
Age (ka)

Figure 2

core SO164-17-2, its condensed succession limits the comparability with the record of MIS 5.

[21] MIS 5 ranges from 160 to 440 cm. A detailed age model was developed for this interval by tuning the benthic isotope record of *Cibicidoides wuellerstorfi* to the global benthic isotope stack LR04 [*Lisiecki and Raymo*, 2005] (Figures 3c and 3d). Sedimentation rates vary between 2.7 and 16 cm/kyr with an average of 5.2 cm/kyrs during MIS 5, with the highest sedimentation rate between 123 and 125 ka at the peak warm stage MIS 5.5. Given that carbonate contents (78.5–87 wt% $CaCO_3$) are relatively stable throughout the record it is likely that the pronounced differences in sedimentation rates are not primarily the effect of productivity changes but point at the highly dynamic nature of the deep currents at Florida Streets affecting sediment accumulation.

3.2. Assessment of Contamination and Diagenetic Effects on the Mg/Ca Ratios

[22] To identify contamination by clay particles and Mn-Fe carbonate and oxide coatings, which might affect the foraminiferal Mg/Ca ratios [*Barker et al.*, 2003], aluminum, iron and manganese concentrations were monitored. Fe/Ca ratios were commonly below 0.1 mmol/mol and therefore indicating that no contamination by detrital material or Fe-rich overgrowth had taken place [*Barker et al.*, 2003]. Mn/Ca ratios were mostly higher than the ratio of 0.1 mmol/mol given by *Barker et al.* [2003] (mean: 0.32 ± 0.09 mmol/mol), but Mn concentrations were an order of magnitude smaller than those of Mg. There is no correlation ($r^2 < 0.01$) between Mn/Ca and Mg/Ca for *G. ruber* (w), which infers that their Mg/Ca ratios are not biased by Fe/Mn coatings. However, a significant correlation of $r^2 = 0.54$ is recognized for *G. crassaformis* (Figure 4), even though the Mn/Ca ratios are on average lower than those of *G. ruber* (w). Calculated $IWT_{Mg/Ca}$ for MIS 5 were on average ~14.0°C, thus considerably warmer than the Holocene values (Figure 2f, see also Data Set S1). Mean Mn/Ca values of MIS 5 (0.25 mmol/mol) are higher by 0.15 mmol/mol than during the Holocene, thus, diagenetic overprinting [see *Barker et al.*, 2003; *Pena et al.*, 2005] by Mn-bearing minerals might have caused a bias toward higher temperatures by contributing additional Mg as a contaminant. Mn-Mg carbonates (kutnahorite) overgrowths as a common source for diagenetic contamination [*Barker et al.*, 2003] usually have Mg/Mn ratios of ca. 0.1 mol/mol [*Barker et al.*, 2003; *Pena et al.*, 2005]. As such, a 0.15 mmol/mol increase in Mn/Ca would contribute to a Mg/Ca increase of only ~0.015 mmol/mol, which is equivalent to a temperature increase by only ~0.07°C. Even the assumption of an unrealistic Mg:Mn ratio of 1:1 in the diagenetic overgrowths would not affect the overall shape of the Mg/Ca curve (presented as Mg/Ca* in Figure 4; Mg/Ca ratios corrected for Mn/Ca). We thus conclude that diagenetic overprinting is not the primary reason for the MIS 1 versus MIS 5 temperature difference and that MIS5 subsurface temperatures were indeed considerably higher than during the Holocene.

[23] Al/Ca ratios of >0.1 mmol/mol are commonly used to detect samples contaminated by clay particles that were not sufficiently removed during the cleaning process [e.g., *Barker et al.*, 2003]. Since Al concentrations are in most samples close to the detection limit of the ICP-OES, we chose to discard samples with Al/Ca ratios >0.15 mmol/mol, because a sufficiently reliable reproducibility (RSD <10%) could only be achieved for samples with correspondingly high Al contents.

[24] Mg/Ca-based temperature reconstructions may yield unrealistic high estimates in case the foraminiferal tests were overgrown by microcrystalline Ca carbonates due to carbonate dissolution and reprecipitation during early diagenesis. *Regenberg et al.* [2007] particularly noted unusual high Mg/Ca ratios >6 mmol/mol in planktic foraminifera (incl. *G. ruber*) in some cores from the Caribbean for MIS 5 and earlier stages. The elevated Mg/Ca ratios were found to go along with reduced Sr/Ca (<1.3 mml/mol) and high $\delta^{18}O$ values, which were both attributed to the chemical composition of the overgrowths. In our record from core SO164-17-2, we note that Sr/Ca ratios of *G. ruber* (w) and *G. crassaformis* are varying in two different ways (Figure 4): *G. ruber* (w) has "normal" Sr/Ca ratios between ~1.4 and ~1.55 mmol/mol also during intervals of Mg/Ca >6 mmol/mol with no similarity to the Mg/Ca record. *G. crassaformis*, on the other hand, has covarying Sr/Ca and Mg/Ca ratios, with Sr/Ca as low as 1.2 mmol/mol but without the inverse relation reported by *Regenberg et al.* [2007]. In fact, a high temperature sensitivity of Sr/Ca ratios of deep dwelling *Globorotalia* species has been found in different studies [*Cléroux et al.*, 2008; *Elderfield et al.*, 2000; *Mortyn et al.*, 2005], which would explain the similarity of the Sr/Ca and Mg/Ca records of *G. crassaformis*. Application of the Sr/Ca temperature equation for *Globorotalia* spp. put forward by *Cléroux et al.* [2008] [$T_{Sr/Ca}$ = (Sr/Ca-1.052(±0.001))/0.0217(±0.021)] (we refer to equation (2) in the main text of *Cléroux et al.* [2008], not the formula given in the abstract

Figure 2. Compilation of data from core SO164-17-2 in comparison to published paleoclimatological and paleoceanographic proxies. (a) NGRIP ice core $\delta^{18}O$ record [*Andersen et al.*, 2004], (b) $\delta^{18}O_{ivf\text{-}sw}$ of *G. crassaformis* (black line) and *G. ruber* (w) (gray line) from SO164-17-2, (c) occurrence of *G. ruber* (w) in a north Atlantic core (M23414; [*Bauch and Kandiano*, 2007]), (d) SST $_{Mg/Ca}$ on *G. ruber* (w) from SO164-17-2, a black bar denoting the average (±1σ) Holocene temperatures, (e) summer (21 June) insolation at 30°N, (f) intermediate water temperatures $IWT_{Mg/Ca}$ from *G. crassaformis* from SO164-17-2, including average Holocene temperatures as a black bar, (g) alkenone SST from Bermuda Rise core MD95–2036 (33°41′N; 57°35′W) [*Lehman et al.*, 2002], (h) benthic $\delta^{13}C$ (*C. wuellerstorfi*) from SO164-17-2, (i) benthic $\delta^{13}C$ from Ceara Rise site EW9209 [*Curry and Oppo*, 1997], and (j) north Atlantic IRD occurrence in core M23414 [*Helmke and Bauch*, 2003]. Indicated are North Atlantic cooling events C19 to C26 [cf. *Chapman and Shackleton*, 1999] in graph A as well as MIS 4 to 6 including substages in the lower *x* axis. Gray bars indicate intermediate water salinity anomalies in Florida Straits, dashed bars mark the climate optimum and deglaciation during MIS 5.5. Error bars denote the standard deviation of replicate analyses, with the exception of the benthic $\delta^{13}C$ record where no replicates were measured; here the long-term analytical precision is given (see section 2).

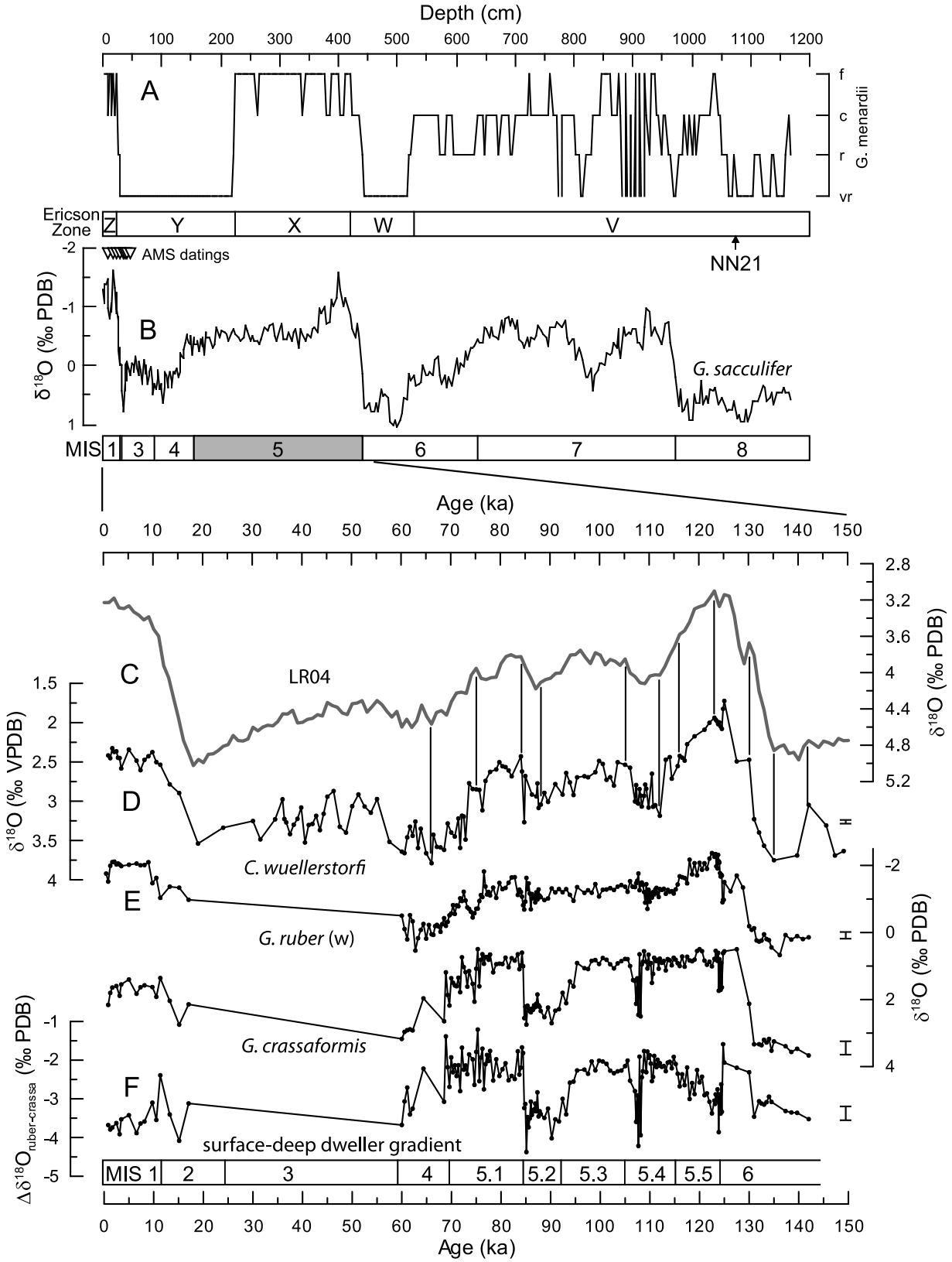
Depth (cm)
A
G. menardii
Ericson Zone
AMS datings
NN21
B
G. sacculifer
MIS
Age (ka)
C
LR04
D
C. wuellerstorfi
E
G. ruber (w)
G. crassaformis
F
surface-deep dweller gradient

Figure 3

(C. Cléroux, personal communication, 2010)) yields temperature estimates not significantly different from that of the Mg/Ca-based calibration after *Regenberg et al.* [2009]. However, we will further use $T_{Mg/Ca}$ since *G. crassaformis* was not included in the Sr/Ca temperature calibration data set of *Cléroux et al.* [2008], and caution has to be taken with the application of this temperature equation prior to the Holocene since the foraminiferal Sr/Ca ratio is prone to influences by other oceanographic parameters such as Sr/Ca changes of the seawater and carbonate saturation [*Cléroux et al.*, 2008; *Elderfield et al.*, 2000; *Mortyn et al.*, 2005].

[25] The dissimilarity between Sr/Ca variations for *G. ruber* and *G. crassaformis* indicates furthermore that diagenetic overgrowth by microcrystalline Ca carbonates apparently does not bias our results as it should affect both species likewise.

[26] A core top study from the Caribbean indicated that dissolution affecting Mg/Ca ratios in water depths only below ~2700 m [*Regenberg et al.*, 2006]. As such, we consider the Mg/Ca ratios to be largely unaffected by dissolution due to the relatively shallow water depth (954 m) and the good aragonite preservation throughout core SO164-17-2.

3.3. Temperature and Salinity Variations

3.3.1. Surface

[27] The SO164-17-2 $SST_{Mg/Ca}$ largely follows the summer insolation at 30°N (Figures 2d and 2e), suggesting that climate variability in Florida Straits is predominately controlled by summer insolation and the expansion of the Atlantic Warm Pool in relation to the summer position of the Intertropical Convergence Zone (ITCZ) [*Ziegler et al.*, 2008]. $SST_{Mg/Ca}$ of SO164-17-2 during MIS 1 (not shown) and MIS 5 is generally 1–3°C higher than those from the Gulf of Mexico and the Caribbean (Figure 5; note that the ODP 999 $SST_{Mg/Ca}$ record was adjusted to account for the different cleaning procedures used and the effects of calcite dissolution as described by *Nürnberg et al.* [2008] and *Regenberg et al.* [2006]). The offset relative to the ODP 999 temperatures can be explained considering the inferred summer bias of $SST_{Mg/Ca}$ in Florida Straits: Mean Holocene temperatures in the Caribbean are ~27.7°C [*Locarnini et al.*, 2006; *Schmidt et al.*, 2004] while the mean summer SST in the Florida Straits is in the range of 29–30°C [*Locarnini et al.*, 2006]. The difference of $SST_{Mg/Ca}$ from SO164-17-2 to the also summer-biased $SST_{Mg/Ca}$ from MD02–2575 [*Ziegler et al.*, 2008] reflects the influence of cool and fresh water derived from the Mississippi and other rivers discharging into the northern Gulf of Mexico. These waters lead to a cooling at water depths between ~20–100 m along the shelf and slope of the northern and eastern Gulf of Mexico [*Locarnini et al.*, 2006]. Integrated for the surface mixed layer, this results in a difference of ~2°C between the sites MD02–2575 and SO164-17-2, which in the range of the offset between the calculated $SST_{Mg/Ca}$.

[28] The $SST_{Mg/Ca}$ increase with the onset of MIS 5.5 occurs very abruptly, with an almost 3°C step toward a short-lived peak with $SST_{Mg/Ca}$ of 32.5°C at 124 ka. The abrupt warming after the end of Termination II is in contrast to the more gradual SST increase observed elsewhere in the Caribbean [*Schmidt et al.*, 2004] and Gulf of Mexico [*Nürnberg et al.*, 2008] (Figure 5). It is unlikely, however, that the unusual abrupt warming in our core is caused by reworking since the benthic foraminiferal $\delta^{18}O$ record does not display any irregular feature that deviates from other benthic oxygen isotope curves (compare Figure 3d). In fact, the rapid $SST_{Mg/Ca}$ warming in SO164-17-2 has a striking similarity with the contemporaneous occurrence of *G. ruber* (w) as an exotic species in core M23414 from the North Atlantic (Figure 2c). It might be suspected that Florida Current and ensuing Gulf Stream strength was particularly enhanced during early MIS 5.5 and facilitated a northward transport of warm and saline water masses entraining *G. ruber* (w). Interestingly, a comparable increase in *G. ruber* (w) abundance in the North Atlantic was not observed during the early Holocene [*Bauch and Kandiano*, 2007], probably as a result of the climatically more favorable conditions during MIS 5.5.

[29] The $\delta^{18}O_{ivf\text{-}sw}$ of surface water, approximating salinity, is relatively constant within error bars during most of MIS 5 and ~1.8‰ (SMOW) lower, indicating less saline conditions than during full glacial MIS 4 and 6 (Figure 2b). After 85 ka, well-expressed fluctuations in the surface and intermediate water $\delta^{18}O_{ivf\text{-}sw}$ occur, resembling the pattern of Dansgaard/Oeschger-like rapid climate oscillations (Figure 2). However, the sample resolution is partly too low to identify all D/O interstadials and stadials. Compared to other $\delta^{18}O_{ivf\text{-}sw}$ reconstructions from MIS 5, Florida Straits values are similar to those from the Gulf of Mexico site MD02–2575 and slightly higher by ~0.5‰ during MIS 5.4 as compared to ODP 999 from the southern Caribbean (Figure 5). Although slightly lower annual mean salinities at ODP 999 than summer salinities in Florida Straits are in accord with the present_day situation [*Antonov et al.*, 2006], a 0.5‰ offset in $\delta^{18}O_{ivf\text{-}sw}$ is within the error bars of the $\delta^{18}O_{ivf\text{-}sw}$ calculations.

3.3.2. Subsurface

[30] Intermediate water $\delta^{18}O_{ivf\text{-}sw}$ of *G. crassaformis* is generally higher by 1.5 to 2‰ during glacial stages MIS 4 and 6 than during most of MIS 5, similar to the surface conditions. However, there are two intervals of markedly

Figure 3. Age model of core SO164-17-2 based on faunal, stable isotope and radiocarbon data; records of Figures 3a and 3b are plotted against depth and Figures 3c–3e against age. (a) Abundance (vr, very rare; r, rare; c, common; f, frequent) of *G. menardii* with indications of the Ericson zones V, W, X, Y, and Z [*Ericson and Wollin*, 1968]; the nannoplankton zone NN21 is indicated by an arrow. (b) The planktic $\delta^{18}O$ record of *G. sacculifer* compared with the inferred Marine Isotope Stages (MIS) 1 to 8 (MIS 2 is too narrow to be indicated); position of AMS ^{14}C datings are shown as triangles. (c) The global benthic $\delta^{18}O$ stack "LR04" from *Lisiecki and Raymo* [2005] which was used to tune the benthic $\delta^{18}O$ curve obtained on *C. wuellerstorfi*. (d) Tie points are indicated by solid lines. (e) The $\delta^{18}O$ values obtained on *G. ruber* (w) and *G. crassaformis*, respectively, are shown for comparison. (f) Gradient $\Delta\delta^{18}O$ between the $\delta^{18}O$ of *G. ruber* (w) and *G. crassaformis*. Note the different scales of the x and y axes. Error bars denote the standard deviation of replicate measurements (for details see section 2).

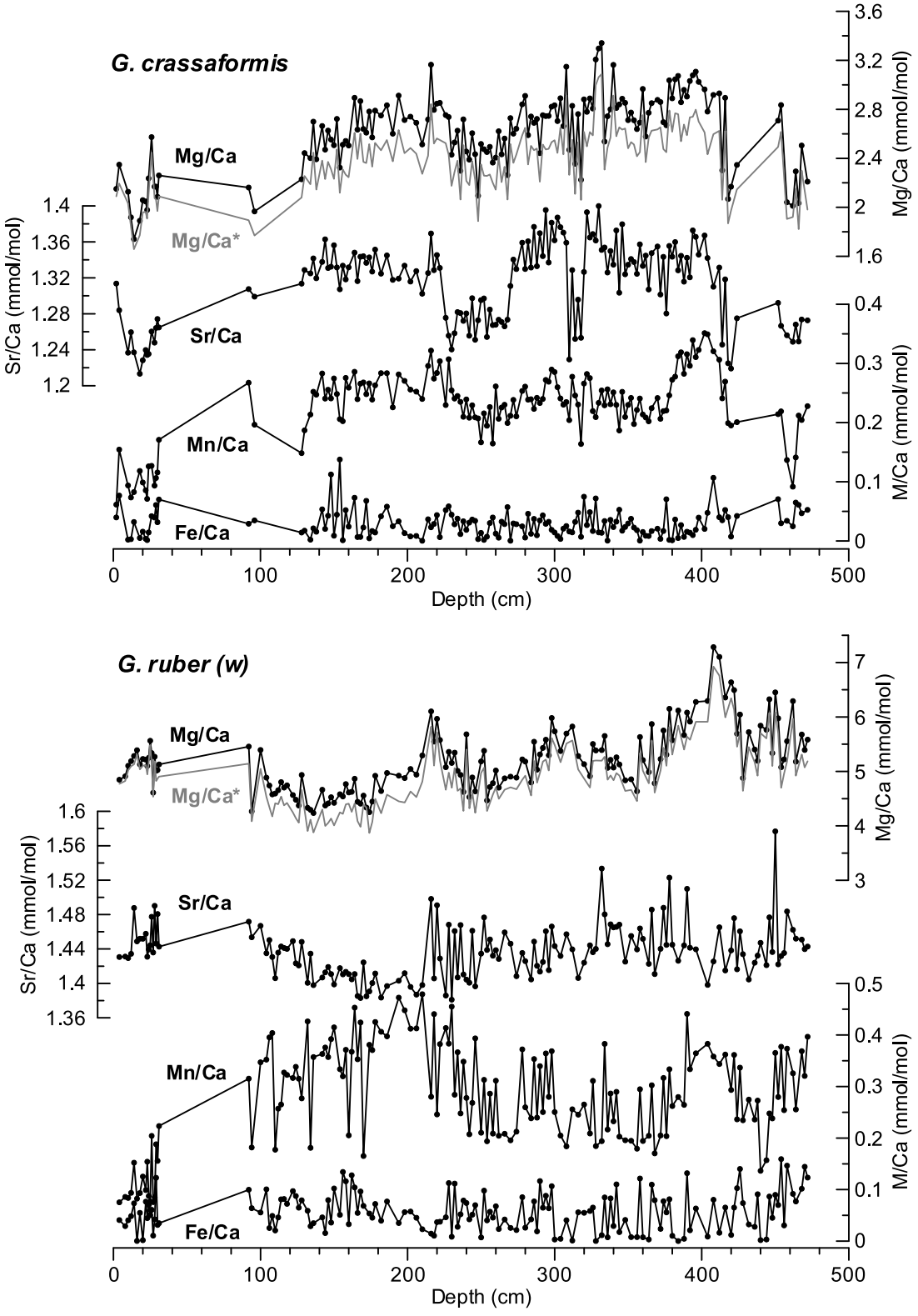

Figure 4. Evaluation of the influence of potential contaminants on the Mg/Ca ratio for (top) *G. crassaformis* and (bottom) for *G. ruber* (w). The ratio Mg/Ca* has been calculated by correcting for Mn-bearing overgrowths using the assumption of a Mn:Mg ratio of 1:1.

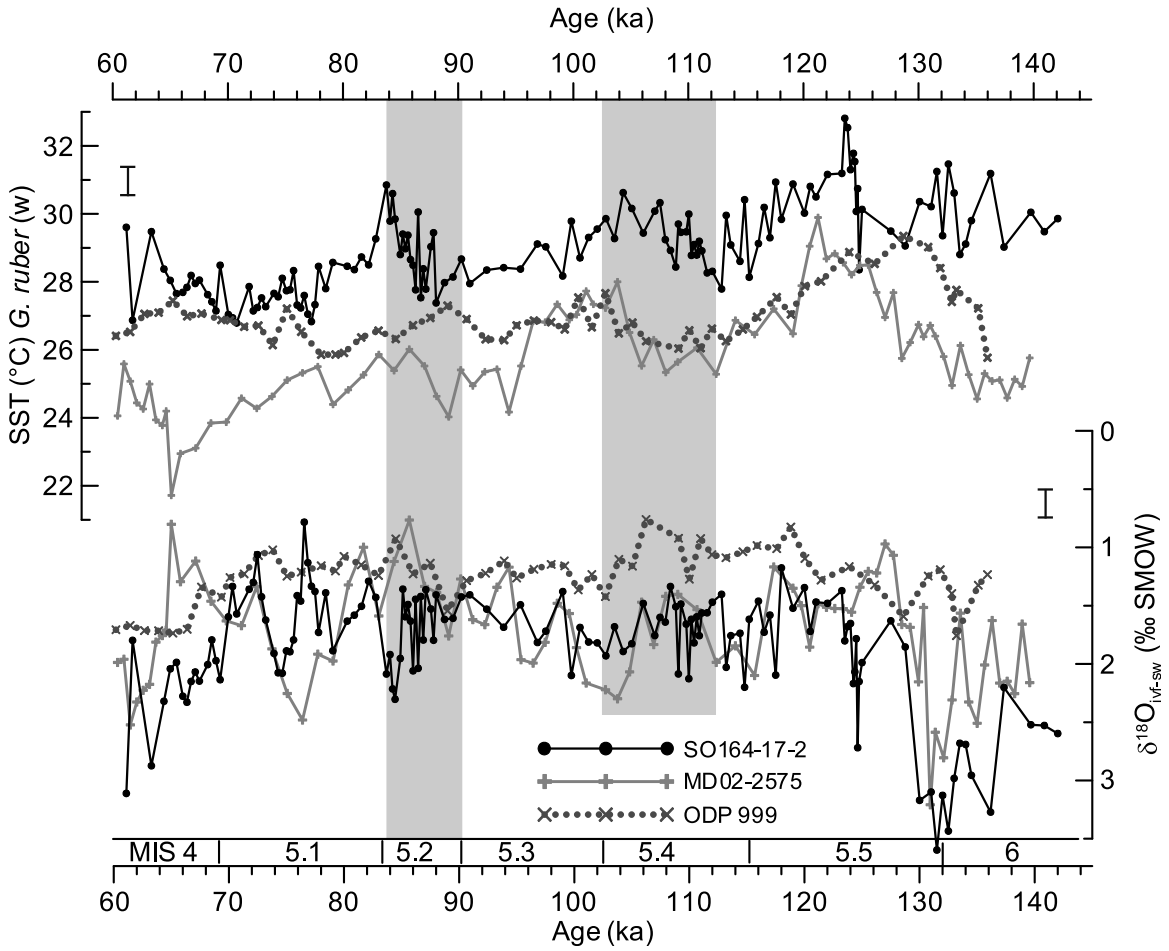

Figure 5. Comparison of SST (top graphs) and $\delta^{18}O_{ivf\text{-}sw}$ (bottom graphs) records from Florida Straits core SO164-17-2 with cores from the NE Gulf of Mexico (MD02–2575) [*Nürnberg et al.*, 2008] and southern central Caribbean (ODP 999) [*Schmidt et al.*, 2004]. Gray bars indicate MIS 5.2 and 5.4. Error bars denote the standard deviation of replicate analyses from SO164-17-2 (see section 2 for details).

elevated intermediate water $\delta^{18}O_{ivf\text{-}sw}$ during MIS 5: a short excursion at the end of MIS 5.4 at ~107 ka, and a more prominent event starting with a gradual increase of $\delta^{18}O_{ivf\text{-}sw}$ at ~94 ka with maximum values throughout MIS 5.2 (from ~85–95 ka). These periods of elevated intermediate water $\delta^{18}O_{ivf\text{-}sw}$ are accompanied by high-amplitude $IWT_{Mg/Ca}$ oscillations at ~107 ka and lowered $IWT_{Mg/Ca}$ during MIS 5.2. $IWT_{Mg/Ca}$ parallels the $SST_{Mg/Ca}$ increase at the beginning of MIS 5.5 but lack the short-lived maximum that is evident in the $SST_{Mg/Ca}$. Notably, the $SST_{Mg/Ca}$ cooling during MIS 5.4 does not affect $IWT_{Mg/Ca}$. The anomalously high $\delta^{18}O_{ivf\text{-}sw}$ values of *G. crassaformis* during MIS 5.2 and at ~107 ka are also expressed as an increased $\delta^{18}O$ gradient between surface and deep dwellers (depicted as $\Delta\delta^{18}O$ in Figure 3f), which is almost as high as during the full glacial intervals of MIS 4 and 6. Following the approach of *Lynch-Stieglitz et al.* [1999b], an enhanced vertical $\delta^{18}O$ gradient represents a more pronounced density gradient between surface and deep water masses, potentially the result of less steeply tilted pycnoclines at the core location (cf. Figure 1d). A decreased pycnocline tilt is then indicative of a reduced vertical shear in the Florida Current and, thus, reduced Gulf Stream strength. A lowered Florida Current strength during cold periods is in accord with the findings of *Lynch-Stieglitz et al.* [1999a] for the Last Glacial Maximum. One remarkable aspect of the $\delta^{18}O$ gradients shown in Figure 3f is that high gradients do not only occur during the cold interglacial phases MIS 5.2, 5.4, 4 and 6, but also during the climatic optimum of MIS 5.5 and the Holocene. Interpreted in terms of density gradients and isopycnal tilt this would indicate reduced Florida Current strength, which is at odds with the assumption of strong throughflow during interglacials and reduced throughflow during glacials [*Lynch-Stieglitz et al.*, 1999a]. However, based on the temperature reconstructions, this offset between $\delta^{18}O$ of *G. ruber* (w) and *G. crassaformis* during MIS 5.5 seems to be caused by the maximum SSTs recorded by *G. ruber* (w) and therefore represents primarily a surface signal not related to geostrophic flow. Hence, although the $\delta^{18}O$ records might imply changes in the density structure of the Florida Straits, we note that based on just one core from the center of the Florida Straits solid inferences about the tilt of isopycnals and Gulf Stream strength cannot be made and remain speculative unless multispecies planktonic foraminiferal oxygen isotope and Mg/Ca records from both sides of Florida Straits will be available.

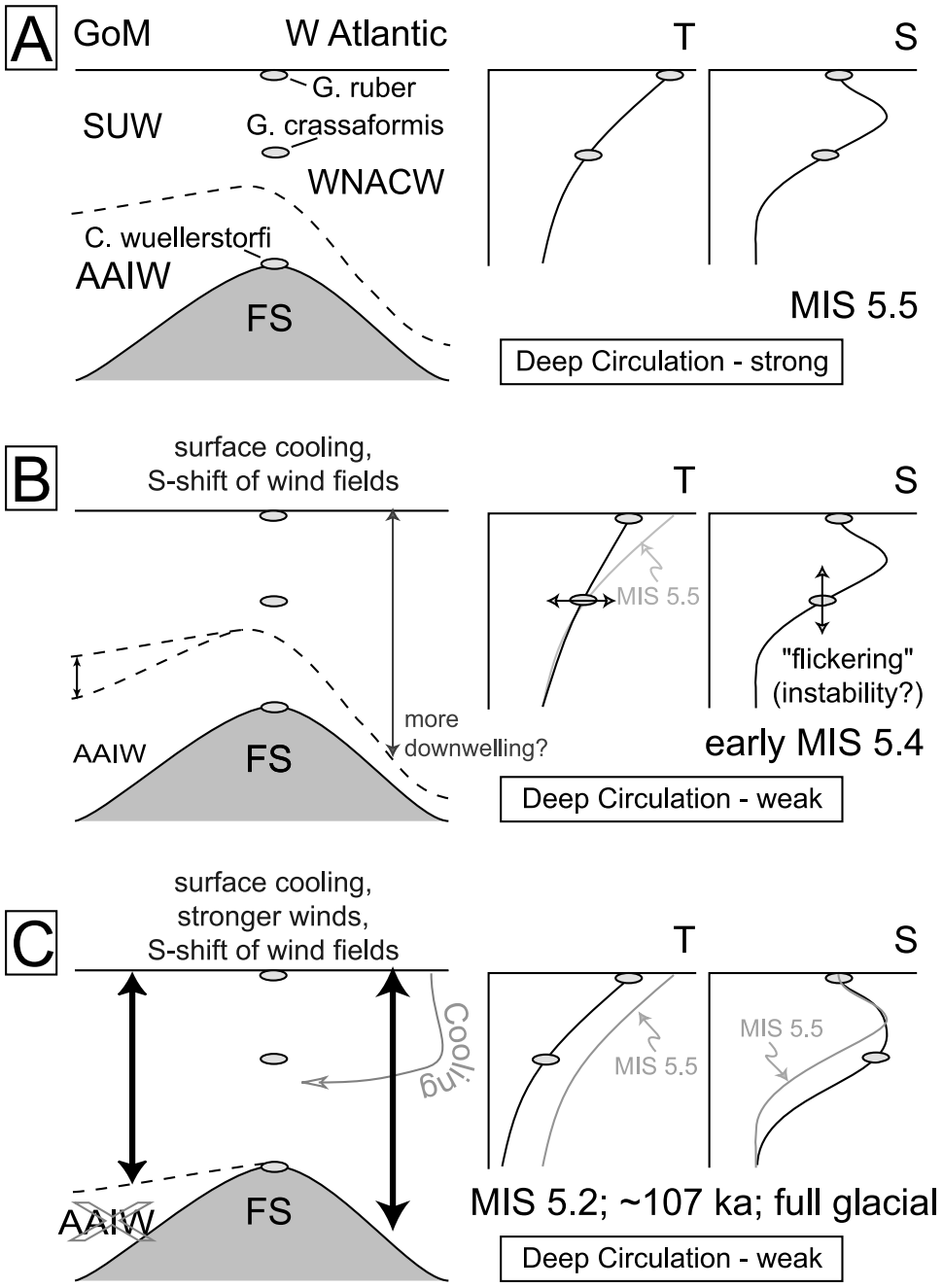

Figure 6. Schematic presentation of different hydrographic states in Florida Straits as inferred from core SO164-17-2. (a) Hydrographic situation during MIS 5.5 with conditions similar to today, i.e., strong deep overturning, AAIW presence and *G. crassaformis* living in less saline conditions than *G. ruber* (supposed calcification depths of the foraminifers are displayed as ellipses; note that Figure 6 is purely schematic and not to scale). (b) Early-to-mid MIS 5.4 is characterized by similar salinity gradients, decreased surface temperatures, and a weakened deep thermohaline circulation. SUW formation is possibly enhanced and AAIW is still present, while intermediate-depth salinities are similar to MIS 5.5. "Flickering" (rapid high-amplitude variations) of $IWT_{Mg/Ca}$ supposedly indicates instable hydrographic conditions. (c) During MIS 5.2, around ~107 ka, and during full glacial conditions SUW is strongly expanded, AAIW is absent, while surface and intermediate depth cooling leads to a shift in the thermocline without altering the temperature gradient. As a consequence of SUW expansion, intermediate-depth salinities increase relative to the MIS 5.5 situation (in gray).

[31] The key issue to be discussed is the origin of the pronounced intermediate depth $\delta^{18}O_{ivf\text{-}sw}$ increases during MIS 5. It seems plausible that intermediate water salinity increases at ~107 ka and during MIS 5.2 as a result of the vertical expansion of highly saline WNACW/SUW waters in Florida Straits (schematically depicted in Figure 6c). However, increasing salinities and decreasing temperatures recorded by *G. crassaformis* during MIS 5.2 and at ~107 ka appear contradictorily, as enhanced vertical SUW extension and WNACW invasion into Florida Straits should have led to higher $IWT_{Mg/Ca}$ (Figure 1b). Intermediate warming is presumably counteracted by widespread wind evaporation–driven surface cooling in the subtropical Atlantic [*Chiang et al.*, 2008], as evidenced by alkenone-derived SSTs in the northern subtropical gyre (Bermuda Rise core MD95–2036, Figure 2g [*Lehman et al.*, 2002]). As subduction of water masses in the subtropical gyre occurs late in winter [*Bryden et al.*, 1996], $IWT_{Mg/Ca}$ in the Florida Straits are generally more similar to the $SST_{alkenone}$ of the gyre region (MD95–2036) and display the same 3–3.5°C amplitude of cooling during MIS 5.2. The proxy evidence is supported by modeling results, which indicate a relative cooling of subsurface water masses in the western (sub)tropical Atlantic north of 20°N as a response to reduced AMOC [*Chang et al.*, 2008].

[32] The combined cooling and salinity increase recorded by *G. crassaformis* basically argues against a change in calcification depth of this species as the primary cause of the proxy variations. According to the current water column structure, an upward migration of *G. crassaformis* to waters with higher salinity would be associated with higher temperatures. Although we cannot exclude that *G. crassaformis* changed its habitat, ongoing studies suggest that this species is rather conservative in its preferred calcification depth at Florida Straits, also during the last deglacial [*Cléroux and Lynch-Stieglitz*, 2010].

[33] Low benthic $\delta^{13}C$ values at ~107 ka and during MIS 5.2 at Ceara Rise site EW9209 [*Curry and Oppo*, 1997] point to a sluggish AMOC during these intervals (Figure 2i). This also coincides with transient periods of continental ice shield growth [e.g., *Chapman and Shackleton*, 1999; *Lisiecki and Raymo*, 2005], as indicated by enhanced portions of ice rafted debris (IRD) in North Atlantic cores [*Chapman and Shackleton*, 1999; *Helmke and Bauch*, 2003] (Figure 2j). In case of the interval at ~107 ka, the $\delta^{13}C$ reduction is expressed as two short-lived intervals where the later at ~106 ka might tentatively be linked to the intermediate $\delta^{18}O_{ivf\text{-}sw}$ anomaly at ~107 ka in the Florida Straits. While this correlation is vague due to the chronostratigraphic uncertainty, the Ceara Rise $\delta^{13}C$ reduction during MIS 5.2 clearly occurs contemporaneously to the high deep dweller $\delta^{18}O_{ivf\text{-}sw}$ values in SO164-17-2. The apparent link between intermediate salt accumulation in the northern subtropical gyre and reduced AMOC strength was also proposed by *Wan et al.* [2010] based on coupled ocean-atmosphere model experiments. While the concept of salt and heat accumulation in the (sub)tropics during reduced overturning is not new [e.g., *Carlson et al.*, 2008; *Schmidt et al.*, 2004, 2006; *Weldeab et al.*, 2006], *Wan et al.* [2010] as well as other studies [*Chang et al.*, 2008; *Chiang et al.*, 2003; *Wan et al.*, 2009; *Zhang*, 2007] point at the rather complex mechanisms that link oceanographic and climatic changes in low latitudes. In case of the western subtropical North Atlantic, lowered precipitation due to the southward shift of the ITCZ was invoked as dominant process [*Chiang et al.*, 2008; *Wan et al.*, 2010], while the reorganization of the oceanic circulation, in particular a reversal of the North Brazil Current, is proposed to be responsible for salt accumulation in the equatorial and southern (sub)tropical Atlantic [*Chang et al.*, 2008; *Wan et al.*, 2010]. Further, intensified wind stress resulting from a more pronounced meridional temperature gradient and stronger northeasterly trade winds might have caused enhanced Ekman downwelling within the subtropical gyre. Increased WNACW production, thus, appears to be a viable mechanism for the westward expansion of saline gyre waters into Florida Straits [*Slowey and Curry*, 1995].

3.4. A Role for AAIW in the Florida Straits During MIS 5?

[34] Considering the synchrony of the atmospheric and oceanographic changes observed during MIS 5.2 and 5.4 it remains speculative why the inferred vertical expansion of the gyre water in Florida Straits is much more pronounced during MIS 5.2 than in 5.4.

[35] In this context the waxing and waning influence of intermediate, southern source waters in the Gulf of Mexico, as for example AAIW, might be an important factor. Records covering the last deglaciation have shown that the formation and northward extent of AAIW was highly variable through time: *Pahnke et al.* [2008] used εNd records from Tobago Basin and Brazil margin to infer that the northward penetration of AAIW was at maximum during Heinrich Event 1 and the Younger Dryas, concomitant to the inferred reduction of the AMOC, but at minimum during the Last Glacial Maximum [*McManus et al.*, 2004]. Benthic Cd/Ca records from Florida Straits, in contrast, argue in favor of a reduced presence of southern source intermediate waters during the same periods of weak AMOC [*Came et al.*, 2008]. The $\delta^{13}C$ data from core SO164-17-2 obtained on the benthic foraminifer *Cibicidoides wuellerstorfi* might serve as an indicator for the relative contribution of southern versus northern source waters, with low $\delta^{13}C$ values indicating a higher contribution of a nutrient-rich southern source. The total benthic $\delta^{13}C$ amplitude of ~0.7‰ during MIS 5 exceeds the 0.32‰ glacial/interglacial $\delta^{13}C$ shift attributed to variations in the global carbon pool [*Duplessy et al.*, 1988]. As profound variations in primary productivity were not recognized, water mass changes remain as a viable explanation for the observed $\delta^{13}C$ variations. Our $\delta^{13}C$ record (Figure 2h) shows the lowest values from Termination II to ~107 ka, which is indicative of the presence of intermediate waters with a high contribution of AAIW-type water in Florida Straits during warmest parts of MIS 5. In turn, the higher $\delta^{13}C$ values prevailing during later stages of MIS 5 would suggest a reduced influence of AAIW. Assuming that diluted AAIW, currently underlying the SUW, was absent after ~107 ka, this would have enabled the SUW to expand to greater depths in Florida Straits (as in MIS 5.2; Figure 6c) during periods of enhanced gyre water production. Instead, at times of larger AAIW contribution, SUW expansion would have been impeded (Figures 6a and 6b). The rapid high-amplitude variations of the $IWT_{Mg/Ca}$ record during MIS 5.2 may therefore be interpreted in terms of a period of hydrographic

instability in Florida Straits (Figure 6b). Based on the available data, the reason for reduced AAIW contribution after ~107 ka remains speculative. Possible mechanisms involve either a generally reduced AAIW production in the source area [*Pahnke and Zahn*, 2005] or a higher amount of subtropical gyre water entering the Caribbean and blocking AAIW intrusion.

[36] While the above discussions center around the impact of high-latitude climatic and oceanographic forcings on the low-latitude hydrography, the apparent expansion of saline water masses in the subtropics might have favored a positive feedback on the invigoration of the thermohaline circulation itself. Previous studies on rapid climatic rebounds, such as the Heinrich and Younger Dryas cooling events, already pinpointed the potential role of (sub)tropical heat and salt accumulation for the resumption of high-latitude deep water formation during periods of a reduced AMOC [*Rühlemann et al.*, 1999; *Schmidt et al.*, 2004, 2006]. Further modeling and proxy studies may show whether the accumulation of a vast amount of highly saline and slightly cooled water in the subsurface of the subtropics have played a similar role in limiting the magnitude of cold events during interglacial MIS 5 during phases of reduced northward heat advection.

4. Conclusions

[37] Combined foraminiferal Mg/Ca and $\delta^{18}O$ data from Florida Straits core SO164-17-2 document abrupt increases in intermediate water salinity at times of transient cooling events during interglacial MIS 5, while surface salinities remained relatively constant. Based on further evidence from benthic $\delta^{13}C$ measurements, we conclude that the intermediate depth salinity anomalies during MIS 5.2 and at ~107 ka probably resulted from independent atmospheric and oceanic forcings, i.e., wind-driven intensification of the subtropical gyre circulation as well as a reduced northward expansion of AAIW. Variations in the $\delta^{18}O$ gradients between deep and shallow dwelling foraminifera indicate that the density structure and in consequence the isopycnal tilt within Florida Straits might have changed during these intervals. The proposed subsurface salinity and temperature variations are broadly in line with paleoceanographic modeling studies and emphasize the sensitivity of the subtropical hydrography to relatively small variations in high- and low-latitude forcings.

[38] **Acknowledgments.** We kindly acknowledge the support and cooperation of captain and crew during R/V *Sonne* Cruise 164 (RASTA). Lulzim Haxhiaj (stable isotope laboratory, IFM-GEOMAR), Karin Kiessling (ICP-OES Laboratory, Kiel University), and Nadine Gehre provided valuable laboratory assistance. The contributions of Hanno Kinkel (Kiel), Jenny Lezius (Bremerhaven), and Jörg Steinlöchner (Stuttgart) to establish the stratigraphy of core SO164-17-2 are gratefully acknowledged. We thank Cyrus Karas, Carsten Eden, and Sascha Flögel for helpful discussions during the progress of this study as well as Editor Chris Charles and two anonymous reviewers for their constructive comments which significantly improved the manuscript. This work has been financed by the German Research Foundation (DFG) in the framework of the German Research Priority Program SPP1266 (INTERDYNAMIK, Project LOOP, Nu 60/17–1).

References

Anand, P., H. Elderfield, and M. H. Conte (2003), Calibration of Mg/Ca thermometry in planktonic forminifera from a sediment trap series, *Paleoceanography*, *18*(2), 1050, doi:10.1029/2002PA000846.

Andersen, K. K., et al. (2004), High-resolution record of Northern Hemisphere climate extending into the last interglacial period, *Nature*, *431*, 147–151, doi:10.1038/nature02805.

Antonov, J. I., R. A. Locarnini, T. P. Boyer, A. V. Mishonov, and H. E. Garcia (2006), *World Ocean Atlas 2005*, vol. 2, *Salinity*, *NOAA Atlas NESDIS*, vol. 62, edited by S. Levitus, 182 pp., NOAA, Silver Spring, Md.

Barker, S., M. Greaves, and H. Elderfield (2003), A study of cleaning procedures used for foraminiferal Mg/Ca paleothermometry, *Geochem. Geophys. Geosyst.*, *4*(9), 8407, doi:10.1029/2003GC000559.

Bauch, H., and E. S. Kandiano (2007), Evidence for early warming and cooling in the North Atlantic surface waters during the last interglacial, *Paleoceanography*, *22*, PA1201, doi:10.1029/2005PA001252.

Bauch, H., H. Erlenkeuser, S. Jung, and J. R. Thiede (2000), Surface and deep water changes in the subpolar North Atlantic during Termination II and the last interglaciation, *Paleoceanography*, *15*(1), 76–84, doi:10.1029/1998PA000343.

Brunner, C. A. (1984), Evidence for increased volume transport of the Florida Current in the Pliocene and Pleistocene, *Mar. Geol.*, *54*(3–4), 223–235, doi:10.1016/0025-3227(84)90039-2.

Brunner, C. A. (1986), Deposition of a muddy sediment drift in the southern Straits of Florida during the late Quaternary, *Mar. Geol.*, *69*(3–4), 235–249, doi:10.1016/0025-3227(86)90041-1.

Bryden, H. L., M. J. Griffiths, A. M. Lavin, R. C. Millard, G. Parrilla, and W. M. Smethie (1996), Decadal changes in water mass characteristics at 24°N in the subtropical North Atlantic Ocean, *J. Clim.*, *9*(12), 3162–3186, doi:10.1175/1520-0442(1996)009<3162:DCIWMC>2.0.CO;2.

Came, R., D. W. Oppo, W. B. Curry, and J. Lynch-Stieglitz (2008), Deglacial variability in the surface return flow of the Atlantic meridional overturning circulation, *Paleoceanography*, *23*, PA1217, doi:10.1029/2007PA001450.

Carlson, A. E., D. W. Oppo, R. E. Came, A. N. LeGrande, L. D. Keigwin, and W. B. Curry (2008), Subtropical Atlantic salinity variability and Atlantic meridional circulation during the last deglaciation, *Geology*, *36*(12), 991–994, doi:10.1130/G25080A.1.

Chang, P., R. Zhang, W. Hazeleger, C. Wen, X. Wan, L. Ji, R. J. Haarsma, W.-P. Breugem, and H. Seidel (2008), Oceanic link between abrupt changes in the North Atlantic Ocean and the African monsoon, *Nat. Geosci.*, *1*, 444–448, doi:10.1038/ngeo218.

Chapman, M. R., and N. J. Shackleton (1999), Global ice-volume fluctuations, North Atlantic ice-rafting events, and deep-ocean circulation changes between 130 and 70 ka, *Geology*, *27*(9), 795–798, doi:10.1130/0091-7613(1999)027<0795:GIVFNA>2.3.CO;2.

Chiang, J. C. H., M. Biasutti, and D. S. Battisti (2003), Sensitivity of the Atlantic Intertropical Convergence Zone to Last Glacial Maximum boundary conditions, *Paleoceanography*, *18*(4), 1094, doi:10.1029/2003PA000916.

Chiang, J. C. H., W. Cheng, and C. M. Bitz (2008), Fast teleconnections to the tropical Atlantic sector from Atlantic thermocline adjustment, *Geophys. Res. Lett.*, *35*, L07704, doi:10.1029/2008GL033292.

Cléroux, C., and J. Lynch-Stieglitz (2010), What caused *G. truncatulinoides* to calcify in shallower water during the early Holocene in the western Atlantic/Gulf of Mexico?, *IOP Conf. Ser. Earth Environ. Sci.*, *9*, 012020, doi:10.1088/1755-1315/9/1/012020.

Cléroux, C., E. Cortijo, P. Anand, L. Labeyrie, F. Bassinot, N. Caillon, and J. C. Duplessy (2008), Mg/Ca and Sr/Ca ratios in planktonic foraminifera: Proxies for upper water column temperature reconstrcution, *Paleoceanography*, *23*, PA3214, doi:10.1029/2007PA001505.

Curry, W. B., and D. W. Oppo (1997), Synchronous, high-frequency oscillations in tropical sea surface temperatures and North Atlantic Deep Water production during the last glacial cycle, *Paleoceanography*, *12*(1), 1–14, doi:10.1029/96PA02413.

Curry, W. B., and D. W. Oppo (2005), Glacial water mass geometry and the distribution of $\delta^{13}C$ of ΣCO_2 in the western Atlantic Ocean, *Paleoceanography*, *20*, PA1017, doi:10.1029/2004PA001021.

Duplessy, J. C., N. J. Shackleton, R. G. Fairbanks, L. Labeyrie, D. W. Oppo, and N. Kallel (1988), Deepwater source variations during the last limatic cycle and their impact on the global deepwater circulation, *Paleoceanography*, *3*(3), 343–360, doi:10.1029/PA003i003p00343.

Elderfield, H., M. Cooper, and G. Ganssen (2000), Sr/Ca in multiple species of planktonic foraminifera: Implications for reconstructions of seawater Sr/Ca, *Geochem. Geophys. Geosyst.*, *1*, 1017, doi:10.1029/1999GC000031.

Elderfield, H., M. J. Vautravers, and M. Cooper (2002), The relationship between shell size and Mg/Ca, Sr/Ca, $\delta^{18}O$, and $\delta^{13}C$ of species of planktonic foraminifera, *Geochem. Geophys. Geosyst.*, *3*(8), 1052, doi:10.1029/2001GC000194.

Ericson, D. B., and G. Wollin (1968), Pleistocene climates and chronology in deep-sea sediments, *Science*, *162*, 1227–1234, doi:10.1126/science.162.3859.1227.

Greaves, M., et al. (2008), Interlaboratory comparison study of calibration standards for foraminiferal Mg/Ca thermometry, *Geochem. Geophys. Geosyst.*, *9*, Q08010, doi:10.1029/2008GC001974.

Haug, G., K. A. Hughen, D. Sigman, L. Peterson, and U. Röhl (2001), Southward migration of the Intertropical Convergence Zone through the Holocene, *Science*, *293*, 1304–1308, doi:10.1126/science.1059725.

Helmke, J. P., and H. Bauch (2003), Comparison of glacial and interglacial conditions between the polar and subpolar North Atlantic region over the last five climatic cycles, *Paleoceanography*, *18*(2), 1036, doi:10.1029/2002PA000794.

Lehman, S. J., J. P. Sachs, A. M. Crotwell, L. D. Keigwin, and E. A. Boyle (2002), Relation of subtropical Atlantic temperature, high-latitude ice rafting, deep water formation, and European climate 130,000–60,000 years ago, *Quat. Sci. Rev.*, *21*(18–19), 1917–1924, doi:10.1016/S0277-3791(02)00078-1.

Lisiecki, L. E., and M. E. Raymo (2005), A Pliocene-Pleistocene stack of 57 globally distributed benthic delta O-18 records, *Paleoceanography*, *20*, PA1003, doi:10.1029/2004PA001071.

Locarnini, R. A., A. V. Mishonov, J. I. Antonov, T. P. Boyer, and H. E. Garcia (2006), *World Ocean Atlas 2005*, vol. 1, *Temperature*, *NOAA Atlas NESDIS*, vol. 61, edited by S. Levitus, 182 pp., NOAA, Silver Spring, Md.

Lund, D. C., J. Lynch-Stieglitz, and W. B. Curry (2006), Gulf Stream density structure and transport during the past millennium, *Nature*, *444*, 601–604, doi:10.1038/nature05277.

Lynch-Stieglitz, J., W. B. Curry, and N. Slowey (1999a), Weaker Gulf Stream in the Florida Straits during the Last Glacial Maximum, *Nature*, *402*, 644–648, doi:10.1038/45204.

Lynch-Stieglitz, J., W. B. Curry, and N. Slowey (1999b), A geostrophic transport estimate for the Florida Current from the oxygen isotope composition of benthic foraminifera, *Paleoceanography*, *14*(3), 360–373, doi:10.1029/1999PA900001.

Lynch-Stieglitz, J., W. B. Curry, and D. C. Lund (2009), Florida Straits density structure and transport over the last 8000 years, *Paleoceanography*, *24*, PA3209, doi:10.1029/2008PA001717.

Martinson, D. G., N. G. Pisias, J. D. Hays, J. Imbrie, T. C. Moore, and N. J. Shackleton (1987), Age dating and the orbital theory of the ice ages: Development of a high-resolution 0 to 300,000-year chronostratigraphy, *Quat. Res.*, *27*(1), 1–29, doi:10.1016/0033-5894(87)90046-9.

McManus, J. F., D. W. Oppo, L. D. Keigwin, J. L. Cullen, and G. C. Bond (2002), Thermohaline circulation and prolonged interglacial warmth in the North Atlantic, *Quat. Res.*, *58*(1), 17–21, doi:10.1006/qres.2002.2367.

McManus, J. F., R. Francois, J.-M. Gherardi, L. D. Keigwin, and S. Brown-Leger (2004), Collapse and rapid resumption of Atlantic meridional circulation linked to deglacial climate changes, *Nature*, *428*, 834–837, doi:10.1038/nature02494.

Mortyn, P. G., H. Elderfield, P. Anand, and M. Greaves (2005), An evaluation of controls on planktonic foraminiferal Sr/Ca: Comparison of water column and core-top data from a North Atlantic transect, *Geochem. Geophys. Geosyst.*, *6*, Q12007, doi:10.1029/2005GC001047.

Nürnberg, D., J. Schönfeld, W. C. Dullo, and C. Rühlemann (2003), RV *Sonne* Cruise report, *Rep. SO164(RASTA)*, 151 pp., GEOMAR, Kiel, Germany.

Nürnberg, D., M. Ziegler, C. Karas, R. Tiedemann, and M. W. Schmidt (2008), Interacting loop current variability and Mississippi River discharge over the past 400 kyr, *Earth Planet. Sci. Lett.*, *272*(1–2), 278–289, doi:10.1016/j.epsl.2008.04.051.

Pahnke, K., and R. Zahn (2005), Southern hemisphere water mass conversion linked with North Atlantic climate variability, *Science*, *307*, 1741–1746, doi:10.1126/science.1102163.

Pahnke, K., S. L. Goldstein, and S. R. Hemming (2008), Abrupt changes in Antarctic Intermediate Water circulation over the past 25,000 years, *Nat. Geosci.*, *1*, 870–874, doi:10.1038/ngeo360.

Pena, L. D., E. Calvo, I. Cacho, S. Eggins, and C. Pelejero (2005), Identification and removal of Mn-Mg-rich contaminant phases on foraminiferal tests: Implications for Mg/Ca past temperature reconstructions, *Geochem. Geophys. Geosyst.*, *6*, Q09P02, doi:10.1029/2005GC000930.

Peterson, L. C., G. H. Haug, R. W. Murray, K. M. Yarincik, J. W. King, T. J. Bralower, K. Kameo, S. D. Rutherford, and R. B. Pearce (2000), Late Quaternary stratigraphy and sedimentation at ODP Site 1002, Cariaco Basin (Venezuela), *Proc. Ocean Drill. Program, Sci. Results*, *165*, 85–99.

Regenberg, M., D. Nürnberg, S. Steph, J. Groeneveld, D. Garbe-Schönberg, R. Tiedemann, and W.-C. Dullo (2006), Assessing the effect of dissolution on planktonic foraminiferal Mg/Ca ratios: Evidence from Caribbean core tops, *Geochem. Geophys. Geosyst.*, *7*, Q07P15, doi:10.1029/2005GC001019.

Regenberg, M., D. Nürnberg, J. Schönfeld, and G.-J. Reichert (2007), Early diagentic overprint in Caribbean sediment cores and its effect on the geochemical composition of planktonic foraminifera, *Biogeosciences*, *4*, 957–973, doi:10.5194/bg-4-957-2007.

Regenberg, M., S. Steph, D. Nürnberg, R. Tiedemann, and D. Garbe-Schönberg (2009), Calibrating Mg/Ca ratios of multiple planktonic foraminiferal species with δ^{18}O-calcification temperatures: Paleothermometry for the upper water column, *Earth Planet. Sci. Lett.*, *278*(3–4), 324–336, doi:10.1016/j.epsl.2008.12.019.

Richardson, W. S., W. J. Schmitz Jr., and P. P. Niiler (1969), The velocity structure of the Florida Current from the Straits of Florida to Cape Fear, *Deep Sea Res. Oceanogr. Abstr.*, *16*, suppl., 225–231.

Rühlemann, C., S. Mulitza, P. J. Müller, G. Wefer, and R. Zahn (1999), Warming of the tropical Atlantic Ocean and slowdown of thermohaline circulation during the last deglaciation, *Nature*, *402*, 511–514, doi:10.1038/990069.

Schmidt, M. W., H. J. Spero, and D. W. Lea (2004), Links between salinity variation in the Caribbean and North Atlantic thermohaline circulation, *Nature*, *428*, 160–163, doi:10.1038/nature02346.

Schmidt, M. W., M. J. Vautravers, and H. J. Spero (2006), Rapid subtropical North Atlantic salinity oscillations across Dansgaard-Oeschger cycles, *Nature*, *443*, 561–564, doi:10.1038/nature05121.

Schmitz, W. J., Jr., and M. S. McCartney (1993), On the North Atlantic Circulation, *Rev. Geophys.*, *31*(1), 29–49, doi:10.1029/92RG02583.

Schmitz, W. J., Jr., and P. L. Richardson (1991), On the sources of the Florida Current, *Deep Sea Res., Part A*, *38*, suppl., S379–S409.

Slowey, N. C., and W. B. Curry (1995), Glacial-interglacial differences in circulation and carbon cycling within the upper western North Atlantic, *Paleoceanography*, *10*(4), 715–732, doi:10.1029/95PA01166.

Steph, S., M. Regenberg, R. Tiedemann, S. Mulitza, and D. Nürnberg (2009), Stable isotopes of planktonic foraminifera from tropical Atlantic/Caribbean core-tops: Implications for reconstructing upper ocean stratification, *Mar. Micropaleontol.*, *71*(1–2), 1–19, doi:10.1016/j.marmicro.2008.12.004.

Thunell, R., E. Tappa, C. Pride, and E. Kincaid (1999), Sea-surface temperature anomalies associated with the 1997–1998 El Nino recorded in the oxygen isotope composition of planktonic foraminifera, *Geology*, *27*(9), 843–846, doi:10.1130/0091-7613(1999)027<0843:SSTAAW>2.3.CO;2.

Waelbroeck, C., L. Labeyrie, E. Michel, J. C. Duplessy, J. F. McManus, K. Lambeck, E. Balbon, and M. Labracherie (2002), Sea-level and deep water temperature changes derived from benthic foraminifera isotopic records, *Quat. Sci. Rev.*, *21*(1–3), 295–305, doi:10.1016/S0277-3791(01)00101-9.

Wan, X., P. Chang, R. Saravanan, R. Zhang, and M. W. Schmidt (2009), On the interpretation of Caribbean paleo-temperature reconstructions during the Younger Dryas, *Geophys. Res. Lett.*, *36*, L02701, doi:10.1029/2008GL035805.

Wan, X., P. Chang, and M. W. Schmidt (2010), Causes of tropical Atlantic paleo-salinity variation during periods of reduced AMOC, *Geophys. Res. Lett.*, *37*, L04603, doi:10.1029/2009GL042013.

Weldeab, S., R. R. Schneider, and M. Kölling (2006), Deglacial sea surface temperature and salinity increase in the western tropical Atlantic in synchrony with high latitude climate instabilities, *Earth Planet. Sci. Lett.*, *241*(3–4), 699–706, doi:10.1016/j.epsl.2005.11.012.

Wüst, G. (1924), Florida- und Antillenstrom: Eine hydrodynamische Untersuchung, *Geogr. Naturwiss. Reihe*, *12*, 1–48.

Zhang, R. (2007), Anticorrelated multidecadal variations between surface and subsurface tropical North Atlantic, *Geophys. Res. Lett.*, *34*, L12713, doi:10.1029/2007GL030225.

Ziegler, M., D. Nürnberg, C. Karas, R. Tiedemann, and L. J. Lourens (2008), Persistent summer expansion of the Atlantic Warm Pool during glacial abrupt cold events, *Nat. Geosci.*, *1*, 601–605, doi:10.1038/ngeo277.

A. Bahr, Institute of Geosciences, University Frankfurt, Altenhöferallee 1, D-60438 Frankfurt am Main, Germany. (a.bahr@em.uni-frankfurt.de)

D. Garbe-Schönberg, Institute of Geosciences, Christian-Albrechts-Universität zu Kiel, Ludewig-Meyn-Str. 10, D-24118 Kiel, Germany.

D. Nürnberg and J. Schönfeld, Leibniz Institute for Marine Sciences IFM-GEOMAR, Wischhofstr. 1-3, D-24148 Kiel, Germany.